Slow heterogeneous relaxation due to constraints in dual XXZ models

Lenart Zadnik[1,*] and Juan P. Garrahan[2,3]

[1] *SISSA and INFN, Via Bonomea 265, 34136 Trieste, Italy*
[2] *School of Physics and Astronomy, University of Nottingham, Nottingham NG7 2RD, United Kingdom*
[3] *Centre for the Mathematics and Theoretical Physics of Quantum Non-Equilibrium Systems, University of Nottingham, Nottingham NG7 2RD, United Kingdom*

With the aim to understand the role of the constraints in the thermalisation of quantum systems, we study the dynamics of a family of kinetically constrained models arising through duality from the XXZ spin chain. We find that integrable and nonintegrable deformations around the stochastic point give rise to ground state phase transitions between localised and delocalised phases, which in turn determine the nature of the relaxation dynamics at finite energy densities. While in the delocalised phase thermalisation is fast and homogeneous, in the localised phase relaxation is slow, temporal autocorrelations exhibit plateaus indicative of metastability, and the growth of entanglement is heterogeneous in space. Furthermore, by considering relaxation from initial product states, we demostrate that this slow thermalisation can be rationalised directly from the presence of constraints in the dynamics.

Introduction. Thermalisation is one of the major challenges to the durability of quantum technologies: quantum coherence—their vital property—cannot be sustained indefinitely due to imperfect isolation from the environment [1–4]. It is also expected to occur in extended isolated systems, where infinitely many degrees of freedom provide an effective bath that leads to equilibration of few-body observables. These attain stationary values predictable by standard statistical ensembles or, in the case of integrable systems with infinitely many conservation laws constraining the dynamics, generalisations thereof [5–8]. In generic systems, where only the energy is conserved, one can understand this in the context of the eigenstate thermalisation hypothesis (ETH). The latter, through a combination of thermodynamic suppression of coherences and dephasing, leads to a drastic reduction in the number of parameters required to describe stationarity [9–12].

While the statistical ensembles can predict the asymptotic expectation values of the few-body observables, they give no information about the time scales over which the relaxation towards them occurs. Speed of relaxation can be affected by various circumstances, such as the extent to which the symmetries of the physical system are broken by the initial conditions [13–15], the presence of emergent quasiconserved quantities [16–20], or dynamical constraints [21–29]. The latter are the main feature of kinetically constrained models (KCM), originally conceived as toy models for slow hierarchical dynamics of classical viscous fluids and glasses [30–33]. Mimicking excluded-volume interactions [34]—a feature of systems extending from supercooled liquids [35, 36] to Rydberg blockade [37, 38]—they can lead to a wide variety of exotic quantum nonequilibrium phenomena that have recently been in the spotlight. Examples include jamming and related Hilbert space fragmentation [39–44], quantum many-body scars (QMBS) [45–48], anomalous transport [49, 50], and cooperative dynamics of fractons [51, 52]. Excluded-volume interactions and dynamical constraints often arise in models with tunable interactions, where strong correlations between excitations are induced in the large coupling limit [37, 41, 53–59]. Alternatively, KCMs can sometimes be related to such models through duality transformations [14, 60–62], an approach we follow here.

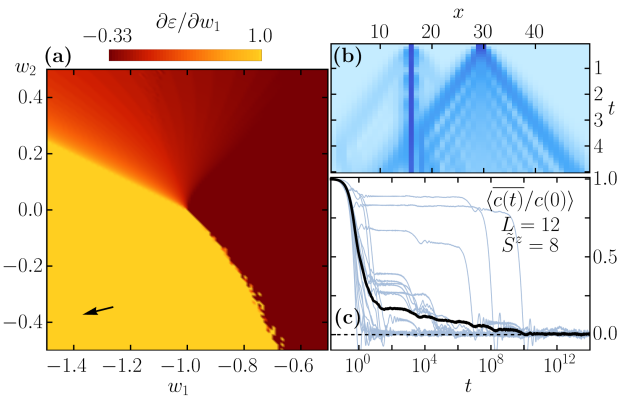

FIG. 1. **Ground state phases and slow relaxation of the XPX model.** (a) Ground state phase diagram of the XPX model in Eq. (1) for $L = 160$ (from DMRG performed using the ITensor library [63, 64]). For smaller $w_{1,2}$ (yellow region) the ground state is localised, while for larger $w_{1,2}$ (red region) it is delocalised. The arrow indicates the values of $w_{1,2}$ used in panels (b,c). (b) Time evolution of a spin configuration $|\cdots\downarrow\cdots\downarrow\downarrow\cdots\rangle$ with dots denoting spins up (from TEBD based on the Armadillo library [65, 66]), for $w_1 = -2, w_2 = -1/2$ in the localised phase. (c) Normalised auto-correlation functions for individual initial configurations (light blue) and their average (black) in the localised phase ($w_1 = -3.5, w_2 = -1.5$), in a specific symmetry sector of the model.

In this paper we consider a family of one-dimensional (1D) quantum models mappable to the anisotropic Heisenberg spin-1/2 chain and its nonintegrable defor-

mation. We investigate two phases of the model depicted in Fig. 1(a): a phase where the ground state is localised (yellow) and one where it is delocalised (red). A striking feature of the model in the phase with a localised ground state is the emergence of facilitated dynamics at finite energy density, as illustrated in Fig. 1(b): certain local arrangements (pairs of spins down, see below) can move freely, whereas certain other isolated excitations remain frozen for long times. We demonstrate the resulting separation of time scales by considering the evolution of temporal autocorrelation functions of particle occupation numbers starting from various initial states—cf. Fig. 1(c). This in turn gives rise to a growth of the bipartite entanglement entropy which is heterogeneous in space, depending on the effect that the dynamical constraints have on spatial fluctuations in initial product states.

Models. We consider a one-dimensional XPX model on a chain of L spins 1/2 with open boundary conditions:

$$H_{\mathrm{XPX}} = \sum_{j=2}^{L-1} \sigma^x_{j-1}(\mathbb{1}-\sigma^z_j)\sigma^x_{j+1} + w_1\sigma^z_j + w_2\sigma^z_{j-1}\sigma^z_{j+1}. \quad (1)$$

Pauli matrices acting in the site j are denoted by σ^α_j, $\alpha \in \{x, y, z\}$, while $\mathbb{1}$ is the identity. The dynamical constraint $\mathbb{1}-\sigma^z_j = 2\,|{\downarrow}\rangle\langle{\downarrow}|_j$ allows the spins in sites $j-1$ and $j+1$ to flip only if a spin down is between them.

When $w_2 = 0$ the XPX model is integrable and belongs to a family of models

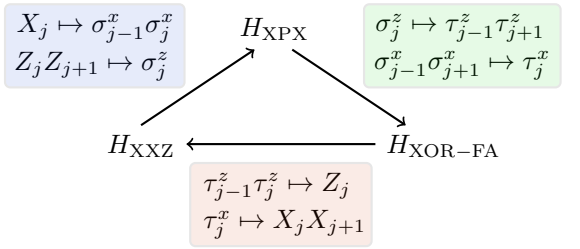

(2)

related by degenerate duality maps often referred to as the bond-site transformations. One of them yields the anisotropic Heisenberg model [14, 60, 62]

$$H_{\mathrm{XXZ}} = \sum_{j=2}^{L-1} X_jX_{j+1} + Y_jY_{j+1} + w_1Z_jZ_{j+1} \quad (3)$$

and the second one the XOR-Fredrickson-Andersen model

$$H_{\mathrm{XOR\text{-}FA}} = \sum_{j=2}^{L-1} \tau^x_j(\mathbb{1} - \tau^z_{j-1}\tau^z_{j+1}) + w_1\tau^z_{j-1}\tau^z_{j+1}, \quad (4)$$

whose kinetic constraint—a quantum XOR gate—allows a spin flip to occur only between two oppositely aligned spins [67]. Operators X_j, Y_j, Z_j, and separately τ^α_j, $\alpha \in \{x, y, z\}$, satisfy Pauli algebra and can be represented as Pauli matrices acting in site j. For $w_2 \neq 0$ the integrability is broken [14]: the corresponding non-integrable deformations are $H_{\mathrm{XXZ}} + w_2\, Z_{j-1}Z_jZ_{j+1}Z_{j+2}$ and $H_{\mathrm{XOR\text{-}FA}} + w_2\, \tau^z_{j-2}\tau^z_{j+2}$.

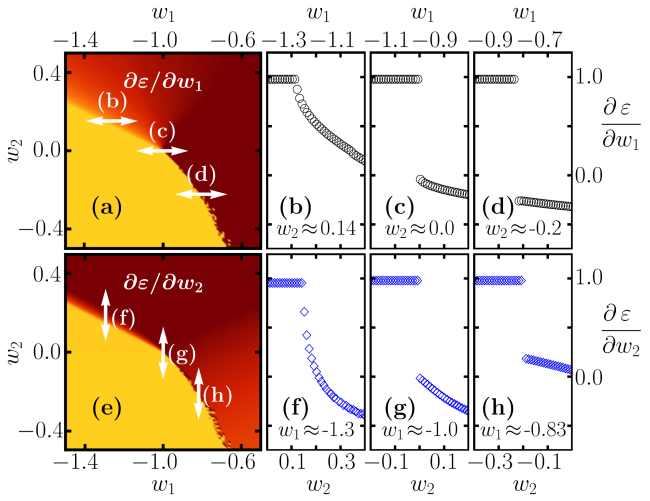

FIG. 2. **Order of ground state phase transitions in the XPX model.** Panels in the first and the second row show the derivatives of the ground state energy on w_1, resp. w_2. For $w_2 \leq 0$ the transition between the localised and the delocalised phase (i.e., between the regions color-coded yellow and red, respectively) is a first-order transition. For $w_2 > 0$ it is of the second order.

We note that there is some freedom in specifying the duality transformations. Choosing $X_j \mapsto \sigma^x_{j-1}\sigma^x_j$, $Y_j \mapsto \sigma^x_{j-1}\sigma^y_j\sigma^z_{j+1}\cdots\sigma^z_L$, $Z_j \mapsto \sigma^z_j\cdots\sigma^z_L$ for $1 \leq j \leq L$, with convention $\sigma^x_0 = 1$, the conserved magnetisation $S^z = \sum_{j=1}^L Z_j$ of the Heisenberg model is mapped into the "semilocal" charge $\tilde{S}^z = \sum_{j=1}^L \sigma^z_j\cdots\sigma^z_L$ of the XPX model: $[H_{\mathrm{XPX}}, \tilde{S}^z] = 0$. Despite not being local, such an operator may crucially affect local relaxation [14, 60].

Notably, all of the models in the family (2) have classical stochastic counterparts. The one for the XPX model with $w_2 = 0$ and $w_1 = -1 - s$ is associated to $\mathbb{W}(s) = -U(H_{\mathrm{XPX}} + (1+s)\mathbb{1})U^{-1}$, where $U = \prod_{j=1}^{L/4}\sigma^z_{4j-1}\sigma^z_{4j}$ and we have assumed $L/4 \in \mathbb{N}$ for convenience. The operator $\mathbb{W}(s=0)$ is a stochastic Markov generator, while for $s \neq 0$ it is a deformed (or "tilted") generator encoding the large deviation (LD) statistics [33, 68, 69] of the number of spin-flips (dynamical activity [70–72]) in trajectories of the dynamics [73].

Via duality to the XXZ model, and up to trivial boundaries, $\mathbb{W}(s=0)$ corresponds to the stochastic generator of the classical *symmetric simple exclusion process* (SSEP) [74], and for $s \neq 0$, it encodes the LDs of the activity in the SSEP [75, 76]. The SSEP is known to have a phase transition in the space of its (long-time) stochastic trajectories between an active and an inactive phase, which shows up as a nonanalyticity at $s = 0$ in

the largest eigenvalue of $\mathbb{W}(s)$ (in the large-size limit) [75–77]. The dynamical LD method [33, 68, 69] provides a means for a statistical ensemble description of trajectories, and the ensuing dynamical phase transition, in the classical stochastic SSEP [75–77]. In the dual picture for the quantum model, this transition (occurring at $w_1 = -1$) corresponds to the ferromagnetic-paraferromagnetic phase transition in the ground state of the XXZ model [78, 79]. In what follows we explore how it affects the relaxation in the XPX model.

Localised and delocalised phases. In the context of quantum dynamics the inactive and active phase of the XPX model will be referred to as the localised and delocalised phase, respectively. Choosing the inverse participation ratio IPR $= \sum_\psi |\langle\psi|\mathrm{GS}\rangle|^4$ as a measure of localisation ($|\mathrm{GS}\rangle$ is the ground state and $|\psi\rangle$ are computational basis states), we indeed find IPR close to one in the former and close to zero in the latter. As shown in Fig. 2 [see also Fig. 1(a)], these two phases extend beyond the integrable line $w_2 = 0$. For all $w_2 \leq 0$ they are separated by a first order transition, both along w_1 as well as w_2. Instead, for $w_2 > 0$ the transition is a second order one, cf. Fig. 2.

An interesting feature of the localised phase, indicated in Fig. 1(b), is what could be described as "fractonic" nature of the excitations [56]: an isolated spin down remains immobile for long times, while two adjacent spins down can move without an energy cost. We note that the isolated spin down in the integrable XPX model ($w_2 = 0$) corresponds to a domain wall in the XXZ model, which does not melt in the $|w_1| > 1$ regime due to being close to a stable kink solution [80–85]. The fractonic dynamics in which particles can move only if paired (assisted hopping) is a sort of dynamical facilitation [32], which can lead to separation of time scales [33]. Remarkably, the resulting metastability exhibited by correlation functions which involve the entire spectrum of H_{XPX}, and which will be explored in the following, is tied to the localisation of the ground state.

Slow relaxation. To probe metastability we consider the average temporal autocorrelation of the one-site occupation number $n_j = (\mathbb{1} + \sigma_j^z)/2$:

$$c_t = \frac{1}{L}\sum_{j=1}^{L} \langle\psi|\, n_j(t) n_j \,|\psi\rangle\,. \tag{5}$$

Here, $n_j(t) = e^{iH_{\mathrm{XPX}}t} n_j e^{-iH_{\mathrm{XPX}}t}$ and $|\psi\rangle$ is a computational basis product state (an eigenstate of all σ_j^z). For such initial states c_t corresponds to the average magnetisation of the initially occupied sites at time t. To smooth out fast fluctuations we furthermore define $\overline{c_t} = t^{-1}\int_0^t \mathrm{d}\tau\, c(\tau)$, which asymptotically approaches the diagonal-ensemble prediction $\overline{c_\infty} = L^{-1}\sum_j \sum_{E_\ell = E_m} \psi_\ell^* \psi_m \langle\ell|\, n_j \,|m\rangle$, the sum over j running over the initially occupied sites only.

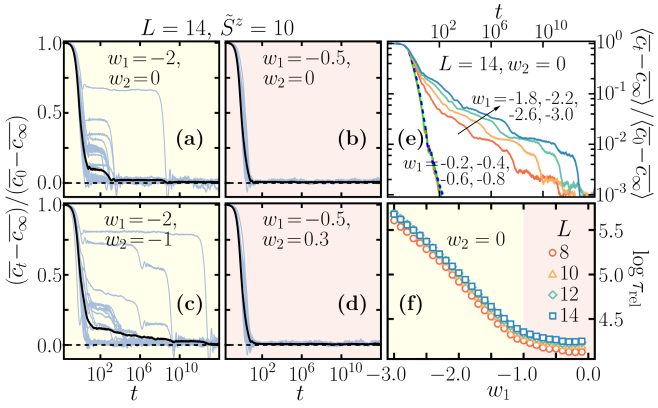

FIG. 3. **Slowdown of the relaxation in the localised phase.** (a-d) Normalised time-integrated autocorrelations $(\overline{c_t} - \overline{c_\infty})/(\overline{c_0} - \overline{c_\infty})$ from initial computational basis states (light blue), and their average over the sector $\tilde{S}^z = L - 4$ (black), for $L = 14$. Panels (a,b) are for the integrable case ($w_2 = 0$), panels (c,d) for the non-integrable one ($w_2 \neq 0$). Panels (a,c) are in the localised phase, panels (b,d) in the delocalised one. (e) Normalised time-integrated correlation $\langle\overline{c_t} - \overline{c_\infty}\rangle$ averaged over all computational basis states (all sectors of Hilbert space). In the delocalised regime (overlapping curves, topmost being dashed) there is almost no w_1 dependence of the relaxation time, while in the localised regime there is a clear slowdown of relaxation with increasing $|w_1|$. The relaxation time seems to obey exponential scaling $\tau_{\mathrm{rel}} \sim \exp(\alpha|w_1 + 1|)$. (f) Estimate of $\log \tau_{\mathrm{rel}}$ from the area under $\langle\overline{c_t} - \overline{c_\infty}\rangle \,/\, \langle\overline{c_0} - \overline{c_\infty}\rangle$ as a function of $\log t$, averaged over the entire Hilbert space.

Panels (a-d) in Fig. 3 portray the autocorrelation functions $(\overline{c_t} - \overline{c_\infty})/(\overline{c_0} - \overline{c_\infty})$, normalised to lie between 0 and 1, for a selection of initial states $|\psi\rangle$ in the semilocal-charge sector $\tilde{S}^z = L - 4$ with $L = 14$. The same panels show also the average of $(\overline{c_t} - \overline{c_\infty})/(\overline{c_0} - \overline{c_\infty})$ over all $|\psi\rangle$ in that sector. In contrast to the delocalised phase, panels (b,d) (red background), where all correlation functions quickly attain stationary values, a large number of correlators in the localised phase, panels (a,c) (yellow background), exhibit plateaus which persist for long times before finally relaxing.

Averaging the correlation function over the initial states reveals a hierarchical decay typical for classical glassy systems, where it is associated with a sequence of different length scales on which relaxation occurs [86–88]. This is most apparent in the autocorrelation $\langle\overline{c_t} - \overline{c_\infty}\rangle \,/\, \langle\overline{c_0} - \overline{c_\infty}\rangle$, where $\langle - \rangle$ is the infinite-temperature average over the entire Hilbert space, plotted in Fig. 3(e). Defining the relaxation time τ_{rel} as the one required by the average correlator to fall below a certain cutoff value ε, there is a clear distinction between the delocalised phase, with no dependence on w_1, and the localised one, for which Fig. 3(e) suggests $\tau_{\mathrm{rel}} \sim e^{\alpha|w_1+1|}$ for some $\alpha > 0$ which may differ between the successive plateaus.

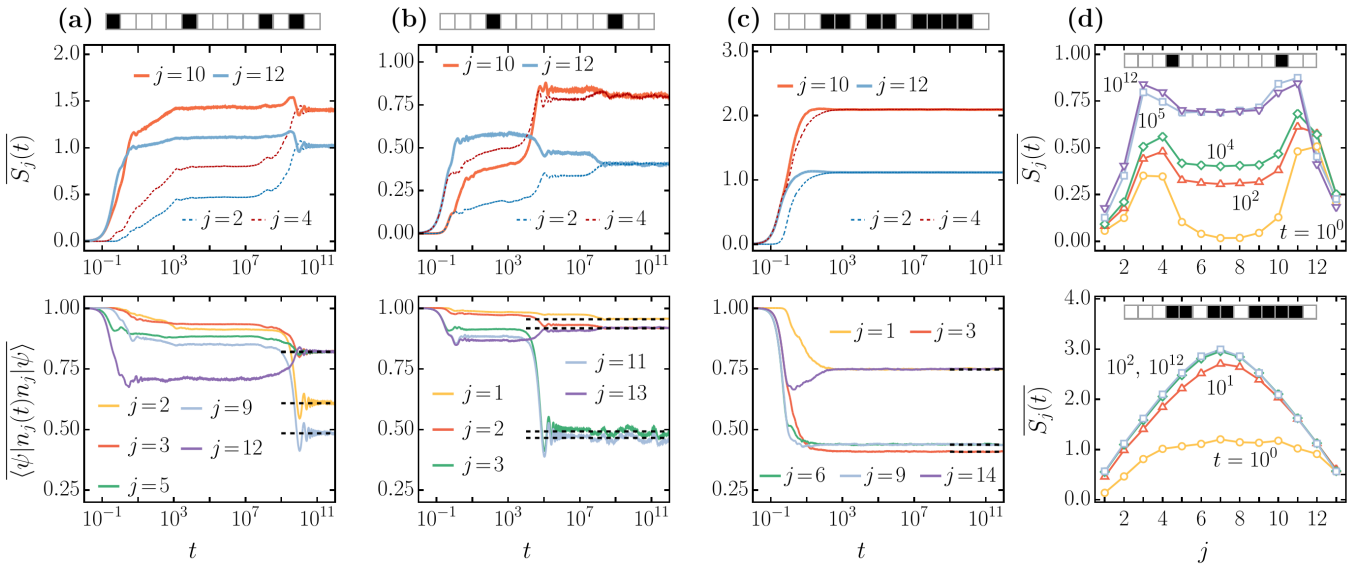

FIG. 4. **Dynamic heterogeneity of the entanglement entropy.** (a-c) Evolution of the time-integrated bipartite entanglement $\overline{S_j(t)}$ (top panels), and the time-integrated temporal autocorrelation of the one-site occupation number $\overline{\langle\psi|\, n_j(t)n_j\,|\psi\rangle}$ (bottom panels), starting from three different initial computational basis states $|\psi\rangle$ (black squares denote spins down, white ones spins up). The plots are for the localised regime of the nonintegrable model with $w_1 = -2, w_2 = -1/2$. (d) Snapshots of the EE profile at different times. The initial configuration for which the time autocorrelations have plateaus indicative of slow relaxation exhibits spatially heterogeneous entanglement evolution. The evolution of EE in the configuration with fast relaxation is instead faster and homogeneous.

An alternative estimate for the relaxation time scale is the area under the averaged correlator in the logarithmic time scale: $\log \tau_{\rm rel} \approx \int_{\log t_{\rm min}}^{\infty} {\rm d}[\log t](\langle \overline{c_t} - \overline{c_\infty}\rangle \,/\, \langle \overline{c_0} - \overline{c_\infty}\rangle)$ [89]. We show this $\tau_{\rm rel}$ in Fig. 3(f) as a function of w_1 ranging between the delocalised and the localised regime of the integrable model ($w_2 = 0$): there is a clear crossover from a regime where $\tau_{\rm rel}$ is only weakly dependent on w_1, coinciding with the delocalised phase (red background), to one of exponential dependence on w_1 in the localised one (yellow background). Note the lack of dependence on system size for the sizes accessible to our numerics. This indicates that relaxation can be slow but not divergent with system size, a typical feature of glassy dynamics.

Note that through duality between the models, cf. Eq. (2), the metastability presented above should occur also for the autocorrelation function of the domain-wall occupation number $(\mathbb{1} - Z_j Z_{j+1})/2$ in the XXZ model, as well as for the autocorrelation function of $(\mathbb{1} - \tau^z_{j-1}\tau^z_{j+1})/2$ in the XOR-FA model.

Large coupling regime. Slow relaxation observed above should be contrasted with the one in the strong coupling limit of the XPX model. In particular, for $w_2 = 0$ and $w_1 \to -\infty$ the dynamics of the XPX model is described by the integrable *dual folded XXZ model* [41, 42, 90]. The latter has an exponentially large sector of jammed states, typical for Rydberg blockade systems [45, 91], and exhibits strong Hilbert space fragmentation [39, 44, 92]. For finite w_1 the dual folded XXZ model accurately describes the time evolution of the XPX model up to times $t \sim |w_1|$. On such time scales the dynamics is confined to small subsectors of Hilbert space and time-averaged correlation functions $\overline{c_t}$ exhibit plateaus. While we have checked that they can be correctly predicted by the folded model's diagonal ensemble, such plateaus are not observed for the values of $w_{1,2}$ considered herein, but instead appear for much larger values of $|w_1|$. Indeed, the plateaus seen in our examples persist on time scales that are exponential and not linear in the parameter. (see Ref. [93] for a perturbative picture of prerelaxation in certain nonintegrable deformations of the XXZ model).

Dynamic heterogeneity in entanglement. Entropy growth provides crucial insight into the role of kinetic constraints in the emergence of metastability [21, 22, 94, 95]. To demonstrate the heterogeneity of dynamical facilitation we consider the bipartite entanglement entropy (EE) $S_j(t) = -{\rm Tr}[\rho_j(\tau)\log\rho_j(\tau)]$, where $\rho_j(t)$ is the time-evolved reduced density matrix of the subsystem consisting of sites $1, 2, \ldots j$. Panels (a-c) of Fig. 4 show $\overline{S_j(t)} = t^{-1}\int_0^t {\rm d}\tau S_j(\tau)$ for several initial states in the localised phase ($w_1 = -2$, $w_2 = -1/2$) of the XPX model on $L = 14$ sites. Figure 4(a) shows the difference between the EE growth when spins down which facilitate relaxation are initially closer (faster EE growth) to when they are further apart (slower EE growth). Note that the heterogeneity of the EE evolution is accompanied by plateaus in the correlators $\overline{\langle\psi|\, n_j(t)n_j\,|\psi\rangle}$. Figure 4(b)

illustrates the interplay of the kinetic term and the three-site potential energy term (for $w_2 \neq 0$): facilitation caused by the spin down closer to the boundary affects less neighbouring sites, which are thus entangled faster by the quantum unitary dynamics, that is, $\overline{S_{12}(t)} \geq \overline{S_2(t)}$ for all t. Finally, due to the assisted hopping in the localised regime, a large density of paired down spins results in a quick equilibration, as shown in Fig. 4(c). The profiles of EE plotted at different times in Fig. 4(d) further corroborate the observation that metastability is associated with dynamic heterogeneity, as is also the case in classical glassy materials with or without quenched disorder [34, 35, 94, 96].

Discussion. We have investigated how metastability and slow heterogeneous relaxation emerge from the kinetic constraints in the XPX spin chain (and by extension in its duals, the XXZ and XOR-FA models). The onset of anomalously slow dynamics coincides with a ground state phase transition from a delocalised to a localised one. This is similar to what occurs in other 1D and 2D constrained models [21, 22, 24, 27] for deformations around their stochastic (frustration free) points. In our case, we also find that the two phases with distinct relaxation extend beyond the range of parameters for which the model is integrable and which include the stochastic point. Interestingly, another contrast to previous results is that the ground state transitions delimiting the two dynamical regimes are not always first-order.

While the models studied herein bear some resemblance to certain KCMs with a variety of low-entangled nonthermalising eigenstates [24, 97], the methods for constructing such states do not straightforwardly generalise here due to crucial differences in either dynamical facilitation, or interaction. Whether the onset of slow heterogeneous dynamics in quantum KCMs is related to nonthermalising states interwoven into the energy spectrum, or the presence of some other exotic symmetries constraining the dynamics [47, 98, 99] remains one of the intriguing open questions.

Acknowledgements. LZ thanks Enej Ilievski for valuable discussions. This work was supported by the ERC under Consolidator grant no. 771536 NEMO (LZ) and Starting grant no. 805252 LoCoMacro (LZ), and by the EPSRC under Grant no. EP/V031201/1 (JPG).

* lzadnik@sissa.it

[1] H. E. Brandt, Qubit devices and the issue of quantum decoherence, Prog. Quantum Electron. **22**, 257 (1999).
[2] J. I. Cirac and P. Zoller, A scalable quantum computer with ions in an array of microtraps, Nature **404**, 579 (2000).
[3] W. H. Zurek, Decoherence, einselection, and the quantum origins of the classical, Rev. Mod. Phys. **75**, 715 (2003).
[4] M. Schlosshauer, Quantum decoherence, Phys. Rep. **831**, 1 (2019).
[5] M. Rigol, V. Dunjko, V. Yurovsky, and M. Olshanii, Relaxation in a completely integrable many-body quantum system: An ab initio study of the dynamics of the highly excited states of 1D lattice hard-core bosons, Phys. Rev. Lett. **98**, 050405 (2007).
[6] E. Ilievski, J. De Nardis, B. Wouters, J.-S. Caux, F. H. L. Essler, and T. Prosen, Complete Generalized Gibbs Ensembles in an Interacting Theory, Phys. Rev. Lett. **115**, 157201 (2015).
[7] C. Gogolin and J. Eisert, Equilibration, thermalisation, and the emergence of statistical mechanics in closed quantum systems, Rep. Prog. Phys. **79**, 056001 (2016).
[8] L. D'Alessio, Y. Kafri, A. Polkovnikov, and M. Rigol, From quantum chaos and eigenstate thermalization to statistical mechanics and thermodynamics, Adv. Phys. **65**, 239 (2016).
[9] J. M. Deutsch, Quantum statistical mechanics in a closed system, Phys. Rev. A **43**, 2046 (1991).
[10] M. Srednicki, Chaos and quantum thermalization, Phys. Rev. E **50**, 888 (1994).
[11] M. Rigol, V. Dunjko, and M. Olshanii, Thermalization and its mechanism for generic isolated quantum systems, Nature **452**, 854 (2008).
[12] J. M. Deutsch, Eigenstate thermalization hypothesis, Rep. Prog. Phys. **81**, 082001 (2018).
[13] V. Alba and M. Fagotti, Prethermalization at low temperature: The scent of long-range order, Phys. Rev. Lett. **119**, 010601 (2017).
[14] M. Fagotti, V. Marić, and L. Zadnik, Nonequilibrium symmetry-protected topological order: emergence of semilocal gibbs ensembles, arXiv:2205.02221 (2022).
[15] F. Ares, S. Murciano, and P. Calabrese, Entanglement asymmetry as a probe of symmetry breaking, Nature Communications **14**, 2036 (2023).
[16] M. Fagotti, On conservation laws, relaxation and pre-relaxation after a quantum quench, J. Stat. Phys. **2014**, P03016 (2014).
[17] B. Bertini and M. Fagotti, Pre-relaxation in weakly interacting models, J. Stat. Mech. **2015**, P07012 (2015).
[18] J. Kemp, N. Y. Yao, C. R. Laumann, and P. Fendley, Long coherence times for edge spins, J. Stat. Mech. **2017**, 063105 (2017).
[19] D. Abanin, W. De Roeck, W. W. Ho, and F. Huveneers, A rigorous theory of many-body prethermalization for periodically driven and closed quantum systems, Comm. Math. Phys. **354**, 809 (2017).
[20] T. Mori, T. N. Ikeda, E. Kaminishi, and M. Ueda, Thermalization and prethermalization in isolated quantum systems: a theoretical overview, J. Phys. B **51**, 112001 (2018).
[21] M. van Horssen, E. Levi, and J. P. Garrahan, Dynamics of many-body localization in a translation-invariant quantum glass model, Phys. Rev. B **92**, 100305 (2015).
[22] Z. Lan, M. van Horssen, S. Powell, and J. P. Garrahan, Quantum slow relaxation and metastability due to dynamical constraints, Phys. Rev. Lett. **121**, 040603 (2018).
[23] A. Morningstar, V. Khemani, and D. A. Huse, Kinetically constrained freezing transition in a dipole-conserving system, Phys. Rev. B **101**, 214205 (2020).
[24] N. Pancotti, G. Giudice, J. I. Cirac, J. P. Garrahan, and M. C. Bañuls, Quantum east model: Localization, nonthermal eigenstates, and slow dynamics, Phys. Rev. X

10, 021051 (2020).
[25] S. Scherg, T. Kohlert, P. Sala, F. Pollmann, B. Hebbe Madhusudhana, I. Bloch, and M. Aidelsburger, Observing non-ergodicity due to kinetic constraints in tilted fermi-hubbard chains, Nature Comm. **12**, 4490 (2021).
[26] P. Brighi, M. Ljubotina, and M. Serbyn, Hilbert space fragmentation and slow dynamics in particle-conserving quantum east models, arXiv:2210.15607 (2022).
[27] R. J. Valencia-Tortora, N. Pancotti, and J. Marino, Kinetically constrained quantum dynamics in superconducting circuits, PRX Quantum **3**, 020346 (2022).
[28] A. Deger, S. Roy, and A. Lazarides, Arresting classical many-body chaos by kinetic constraints, Phys. Rev. Lett. **129**, 160601 (2022).
[29] A. Deger, A. Lazarides, and S. Roy, Constrained dynamics and directed percolation, Phys. Rev. Lett. **129**, 190601 (2022).
[30] R. G. Palmer, D. L. Stein, E. Abrahams, and P. W. Anderson, Models of hierarchically constrained dynamics for glassy relaxation, Phys. Rev. Lett. **53**, 958 (1984).
[31] G. H. Fredrickson and H. C. Andersen, Kinetic ising model of the glass transition, Phys. Rev. Lett. **53**, 1244 (1984).
[32] F. Ritort and P. Sollich, Glassy dynamics of kinetically constrained models, Adv. Phys. **52**, 219 (2003).
[33] J. P. Garrahan, Aspects of non-equilibrium in classical and quantum systems: Slow relaxation and glasses, dynamical large deviations, quantum non-ergodicity, and open quantum dynamics, Physica A **504**, 130 (2018).
[34] D. Chandler and J. P. Garrahan, Dynamics on the way to forming glass: Bubbles in space-time, Annu. Rev. Phys. Chem. **61**, 191 (2010).
[35] L. Berthier and G. Biroli, Theoretical perspective on the glass transition and amorphous materials, Rev. Mod. Phys. **83**, 587 (2011).
[36] G. Biroli and J. P. Garrahan, Perspective: The glass transition, J. Chem. Phys. **138**, 12A301 (2013).
[37] I. Lesanovsky, Many-Body spin interactions and the ground state of a dense Rydberg lattice gas, Phys. Rev. Lett. **106**, 025301 (2011).
[38] A. Browaeys and T. Lahaye, Many-body physics with individually controlled Rydberg atoms, Nature Phys. **16**, 132 (2020).
[39] Z.-C. Yang, F. Liu, A. V. Gorshkov, and T. Iadecola, Hilbert-space fragmentation from strict confinement, Phys. Rev. Lett. **124**, 207602 (2020).
[40] C. M. Langlett and S. Xu, Hilbert space fragmentation and exact scars of generalized Fredkin spin chains, Phys. Rev. B **103**, L220304 (2021).
[41] L. Zadnik and M. Fagotti, The folded spin-1/2 XXZ model: I. Diagonalisation, jamming, and ground state properties, SciPost Phys. Core **4**, 010 (2021).
[42] B. Pozsgay, T. Gombor, A. Hutsalyuk, Y. Jiang, L. Pristyák, and E. Vernier, Integrable spin chain with Hilbert space fragmentation and solvable real-time dynamics, Phys. Rev. E **104**, 044106 (2021).
[43] K. Tamura and H. Katsura, Quantum many-body scars of spinless fermions with density-assisted hopping in higher dimensions, Phys. Rev. B **106**, 144306 (2022).
[44] K. Bidzhiev, M. Fagotti, and L. Zadnik, Macroscopic effects of localized measurements in jammed states of quantum spin chains, Phys. Rev. Lett. **128**, 130603 (2022).
[45] H. Bernien, S. Schwartz, A. Keesling, H. Levine, A. Omran, H. Pichler, S. Choi, A. S. Zibrov, M. Endres, M. Greiner, V. Vuletić, and M. D. Lukin, Probing many-body dynamics on a 51-atom quantum simulator, Nature **551**, 579 (2017).
[46] C. J. Turner, A. A. Michailidis, D. A. Abanin, M. Serbyn, and Z. Papić, Weak ergodicity breaking from quantum many-body scars, Nature Phys. **14**, 745 (2018).
[47] S. Moudgalya, B. A. Bernevig, and N. Regnault, Quantum many-body scars and Hilbert space fragmentation: a review of exact results, Rep. Prog. Phys. **85**, 086501 (2022).
[48] D. Bluvstein, A. Omran, H. Levine, A. Keesling, G. Semeghini, S. Ebadi, T. T. Wang, A. A. Michailidis, N. Maskara, W. W. Ho, S. Choi, M. Serbyn, M. Greiner, V. Vuletić, and M. D. Lukin, Controlling quantum many-body dynamics in driven Rydberg atom arrays, Science **371**, 1355 (2021).
[49] Z.-C. Yang, Distinction Between Transport and Rényi Entropy Growth in Kinetically Constrained Models, arXiv:2208.07480 (2022).
[50] M. Ljubotina, J.-Y. Desaules, M. Serbyn, and Z. Papić, Superdiffusive energy transport in kinetically constrained models, Phys. Rev. X **13**, 011033 (2023).
[51] R. M. Nandkishore and M. Hermele, Fractons, Ann. Rev. Condens. Matter **10**, 295 (2019).
[52] M. Pretko, X. Chen, and Y. You, Fracton phases of matter, Int. J. Mod. Phys. A **35**, 2030003 (2020).
[53] A. Izergin, A. Pronko, and N. Abarenkova, Temperature correlators in the one-dimensional Hubbard model in the strong coupling limit, Phys. Lett. A **245**, 537 (1998).
[54] N. I. Abarenkova and A. G. Pronko, Temperature correlation function in the absolutely anisotropic XXZ Heisenberg magnet, Theor. Math. Phys. **131**, 690 (2002).
[55] N. M. Bogoliubov and C. L. Malyshev, Ising limit of a Heisenberg XXZ magnet and some temperature correlation functions, Theor. Math. Phys. **169**, 1517 (2011).
[56] S. Pai and M. Pretko, Fractons from confinement in one dimension, Phys. Rev. Res. **2**, 013094 (2020).
[57] U. Borla, R. Verresen, F. Grusdt, and S. Moroz, Confined phases of one-dimensional spinless fermions coupled to Z_2 gauge theory, Phys. Rev. Lett. **124**, 120503 (2020).
[58] E. Tartaglia, P. Calabrese, and B. Bertini, Real-time evolution in the Hubbard model with infinite repulsion, SciPost Phys. **12**, 028 (2022).
[59] A. Bastianello, U. Borla, and S. Moroz, Fragmentation and emergent integrable transport in the weakly tilted Ising chain, Phys. Rev. Lett. **128**, 196601 (2022).
[60] M. Fagotti, Global quenches after localized perturbations, Phys. Rev. Lett. **128**, 110602 (2022).
[61] N. G. Jones and N. Linden, Integrable spin chains and the Clifford group, J. Mat. Phys. **63**, 101901 (2022).
[62] L. Eck and P. Fendley, From the XXZ chain to the integrable Rydberg-blockade ladder via non-invertible duality defects, arXiv:2302.14081 (2023).
[63] M. Fishman, S. R. White, and E. M. Stoudenmire, The ITensor software library for tensor network calculations, SciPost Phys. Codebases , 4 (2022).
[64] M. Fishman, S. R. White, and E. M. Stoudenmire, Codebase release 0.3 for ITensor, SciPost Phys. Codebases , 4 (2022).
[65] C. Sanderson and R. Curtin, Armadillo: a template-based c++ library for linear algebra, J. Open Source Softw. **1**, 26 (2016).
[66] C. Sanderson and R. Curtin, A user-friendly hybrid

sparse matrix class in c++, in *Mathematical Software – ICMS 2018*, edited by J. H. Davenport, M. Kauers, G. Labahn, and J. Urban (Springer International Publishing, Cham, 2018) pp. 422–430.

[67] L. Causer, I. Lesanovsky, M. C. Bañuls, and J. P. Garrahan, Dynamics and large deviation transitions of the XOR-Fredrickson-Andersen kinetically constrained model, Phys. Rev. E **102**, 052132 (2020).

[68] H. Touchette, The large deviation approach to statistical mechanics, Phys. Rep. **478**, 1 (2009).

[69] R. L. Jack, Ergodicity and large deviations in physical systems with stochastic dynamics, Eur. Phys. J. B **93**, 74 (2020).

[70] V. Lecomte, C. Appert-Rolland, and F. van Wijland, Chaotic properties of systems with Markov dynamics, Phys. Rev. Lett. **95**, 010601 (2005).

[71] V. Lecomte, C. Appert-Rolland, and F. van Wijland, Thermodynamic formalism for systems with Markov dynamics, J. Stat. Phys. **127**, 51 (2007).

[72] J. P. Garrahan, R. L. Jack, V. Lecomte, E. Pitard, K. van Duijvendijk, and F. van Wijland, First-order dynamical phase transition in models of glasses: an approach based on ensembles of histories, J. Phys. A **42**, 075007 (2009).

[73] For $w_1, w_2 \neq 0$, the operator (1) is the tilted generator that encodes the joint statistics of two trajectory observables, $-\int_t \sum_j \sigma_j^z$, corresponding to the integrated escape rate and therefore the activity [72], and $-\int_t \sum_j \sigma_{j-1}^z \sigma_{j+1}^z$. .

[74] O. Golinelli and K. Mallick, The asymmetric simple exclusion process: an integrable model for non-equilibrium statistical mechanics, J. Phys. A **39**, 12679 (2006).

[75] C. Appert-Rolland, B. Derrida, V. Lecomte, and F. van Wijland, Universal cumulants of the current in diffusive systems on a ring, Phys. Rev. E **78**, 021122 (2008).

[76] R. L. Jack, I. R. Thompson, and P. Sollich, Hyperuniformity and phase separation in biased ensembles of trajectories for diffusive systems, Phys. Rev. Lett. **114**, 060601 (2015).

[77] V. Lecomte, J. P. Garrahan, and F. van Wijland, Inactive dynamical phase of a symmetric exclusion process on a ring, J. Phys. A **45**, 175001 (2012).

[78] J. Des Cloizeaux and M. Gaudin, Anisotropic linear magnetic chain, J. Mat. Phys. **7**, 1384 (1966).

[79] C. N. Yang and C. P. Yang, One-dimensional chain of anisotropic spin-spin interactions. II. Properties of the ground-state energy per lattice site for an infinite system, Phys. Rev. **150**, 327 (1966).

[80] T. Koma and B. Nachtergaele, The complete set of ground states of the ferromagnetic XXZ chains, ATMP **2**, 533 (1998).

[81] D. Gobert, C. Kollath, U. Schollwöck, and G. Schütz, Real-time dynamics in spin-$\frac{1}{2}$ chains with adaptive time-dependent density matrix renormalization group, Phys. Rev. E **71**, 036102 (2005).

[82] J. Mossel and J.-S. Caux, Relaxation dynamics in the gapped XXZ spin-1/2 chain, New J. Phys. **12**, 055028 (2010).

[83] G. Misguich, K. Mallick, and P. L. Krapivsky, Dynamics of the spin-$\frac{1}{2}$ Heisenberg chain initialized in a domain-wall state, Phys. Rev. B **96**, 195151 (2017).

[84] O. Gamayun, Y. Miao, and E. Ilievski, Domain-wall dynamics in the Landau-Lifshitz magnet and the classical-quantum correspondence for spin transport, Phys. Rev. B **99**, 140301(R) (2019).

[85] G. Misguich, N. Pavloff, and V. Pasquier, Domain wall problem in the quantum XXZ chain and semiclassical behavior close to the isotropic point, SciPost Phys. **7**, 025 (2019).

[86] P. Sollich and M. R. Evans, Glassy time-scale divergence and anomalous coarsening in a kinetically constrained spin chain, Phys. Rev. Lett. **83**, 3238 (1999).

[87] D. J. Ashton, L. O. Hedges, and J. P. Garrahan, Fast simulation of facilitated spin models, J. Stat. Mech. **2005**, P12010 (2005).

[88] A. S. Keys, L. O. Hedges, J. P. Garrahan, S. C. Glotzer, and D. Chandler, Excitations are localized and relaxation is hierarchical in glass-forming liquids, Phys. Rev. X **1**, 021013 (2011).

[89] We choose the short-time cutoff $t_{\min} = 10^{-2}$, but this value does not affect the estimation of the relaxation time.

[90] L. Zadnik, K. Bidzhiev, and M. Fagotti, The folded spin-1/2 XXZ model: II. Thermodynamics and hydrodynamics with a minimal set of charges, SciPost Phys. **10**, 099 (2021).

[91] I. Lesanovsky and H. Katsura, Interacting Fibonacci anyons in a Rydberg gas, Phys. Rev. A **86**, 041601(R) (2012).

[92] L. Zadnik, S. Bocini, K. Bidzhiev, and M. Fagotti, Measurement catastrophe and ballistic spread of charge density with vanishing current, J. Phys. A **55**, 474001 (2022).

[93] A. A. Michailidis, M. Žnidarič, M. Medvedyeva, D. A. Abanin, T. Prosen, and Z. Papić, Slow dynamics in translation-invariant quantum lattice models, Phys. Rev. B **97**, 104307 (2018).

[94] J. P. Garrahan and D. Chandler, Geometrical explanation and scaling of dynamical heterogeneities in glass forming systems, Phys. Rev. Lett. **89**, 035704 (2002).

[95] M. Merolle, J. P. Garrahan, and D. Chandler, Space–time thermodynamics of the glass transition, Proc. Natl. Acad. Sci. USA **102**, 10837 (2005).

[96] L. Berthier, G. Biroli, J.-P. Bouchaud, L. Cipelletti, and W. van Saarloos, *Dynamical heterogeneities in glasses, colloids, and granular media*, Vol. 150 (OUP Oxford, 2011).

[97] T. Iadecola and M. Schecter, Quantum many-body scar states with emergent kinetic constraints and finite-entanglement revivals, Phys. Rev. B **101**, 024306 (2020).

[98] B. Buča, Unified theory of local quantum many-body dynamics: Eigenoperator thermalization theorems, arXiv:2301.07091 (2023).

[99] M. Borsi, L. Pristyák, and B. Pozsgay, Matrix product symmetries and breakdown of thermalization from hard rod deformations, arXiv:2302.07219 (2023).